NASA TECHNICAL MEMORANDUM

NASA-TM-X-1342

PRELIMINARY TESTS OF INSULATED ACCELERATOR GRID FOR ELECTRON-BOMBARDMENT THRUSTOR

by Paul M. Margosian

Lewis Research Center

Cleveland, Ohio

NATIONAL AERONAUTICS AND SPACE ADMINISTRATION • WASHINGTON, D. C. • FEBRUARY 1967

NASA TM X-1342

PRELIMINARY TESTS OF INSULATED ACCELERATOR GRID FOR ELECTRON-BOMBARDMENT THRUSTOR

By Paul M. Margosian

Lewis Research Center
Cleveland, Ohio

NATIONAL AERONAUTICS AND SPACE ADMINISTRATION

For sale by the Clearinghouse for Federal Scientific and Technical Information
Springfield, Virginia 22151 – Price $1.00

PRELIMINARY TESTS OF INSULATED ACCELERATOR GRID FOR ELECTRON-BOMBARDMENT THRUSTOR

by Paul M. Margosian

Lewis Research Center

SUMMARY

An electron-bombardment ion thrustor was operated with a single, insulated accelerator grid. Grids were made of drilled metal plates coated with a thin layer of ceramic, drilled ceramic plates coated with a thin layer of metal, and match-drilled plates of ceramic and metal bolted together. The insulating material separated the plasma in the ion chamber from the negatively biased accelerator grid, and thus eliminated the positively biased "screen" grid normally used for this purpose. Operation was possible at net accelerating voltages of 400 to 4000 volts. The ion-chamber power required per beam ion was reduced by a factor of 2 or more from that obtained with conventional grids.

INTRODUCTION

During the past few years, most of the components of the electron-bombardment ion thrustor have been studied at length and have been steadily improved. One basic component that has been highly developed is the system of grids that accelerates ions out of the thrustor. The usual grid system consists of a pair of match-drilled stainless-steel or molybdenum plates. The effects of hole size, grid thickness, grid separation, percent of open area, etc., have been studied experimentally (refs. 1 to 3) and, to a limited degree, theoretically (ref. 4).

In a recent report on the operation of an ion thrustor with a radiofrequency discharge (ref. 5), a way to eliminate the screen grid was described. A drilled, quartz grid plate was placed on the discharge-chamber side of the accelerator grid and was used to shield the accelerator grid from direct impingement of ions. Ions were probably extracted from the discharge chamber through a curved sheath that formed in the vicinity of each hole, just as it does for a conventional pair of grids.

If the metallic screen grid could be eliminated from the accelerator system, the range of operation of the electron-bombardment ion thrustor might be extended and fabrication of the grids could be simplified. One use of the thrustor might be space

operation at several hundred volts net accelerating potential, which could permit direct coupling to lower voltage power systems, such as solar-cell arrays. Without the conventional screen, an accelerator could be constructed with a high perveance by using many small holes and a short accelerating length (corresponding to the thickness of the ceramic layer). The design and fabrication of large accelerator grids would also be possible. Such grids have alinement problems because of both a large ratio of unsupported span to grid separation and the differential thermal expansion of the grids.

Tests were conducted to provide a description of the experimental performance of a single ceramic-protected metallic accelerator grid operated as a component of a direct-current electron-bombardment thrustor. For comparison, data are also presented on the operation of the conventional grid system.

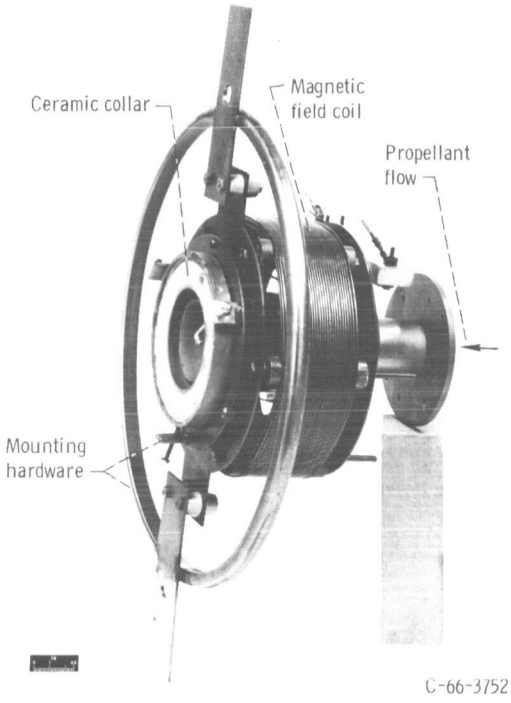

Figure 1. - The 5-centimeter-diameter ion thrustor used for tests. Accelerator grid removed.

SYMBOLS

B	magnetic field strength, T
J_A	accelerator current, A
J_B	ion beam current, A
J_E	emission current, A
J_F	filament-heating current, A
J_M	magnetic field solenoid current, A
J_N	neutral propellant flow rate, equivalent A
J_{SD}	screen and distributor current, A
V_A	accelerator voltage, V
V_I	net accelerating voltage, V
ΔV_I	discharge voltage, V
η_u	propellant-utilization efficiency, percent

APPARATUS

Tests were conducted in a 1.5-meter-diameter by 5-meter-long vacuum tank capable of pressures in the range of 10^{-6} torr. A detailed description of this facility is given in reference 6. The ion thrustor used in most of the tests was the 5-centimeter-diameter model (ref. 7) shown in figure 1. The propellant, mercury, was fed into the thrustor from a vaporizer through a calibrated orifice. The ion-chamber standard cathode con-

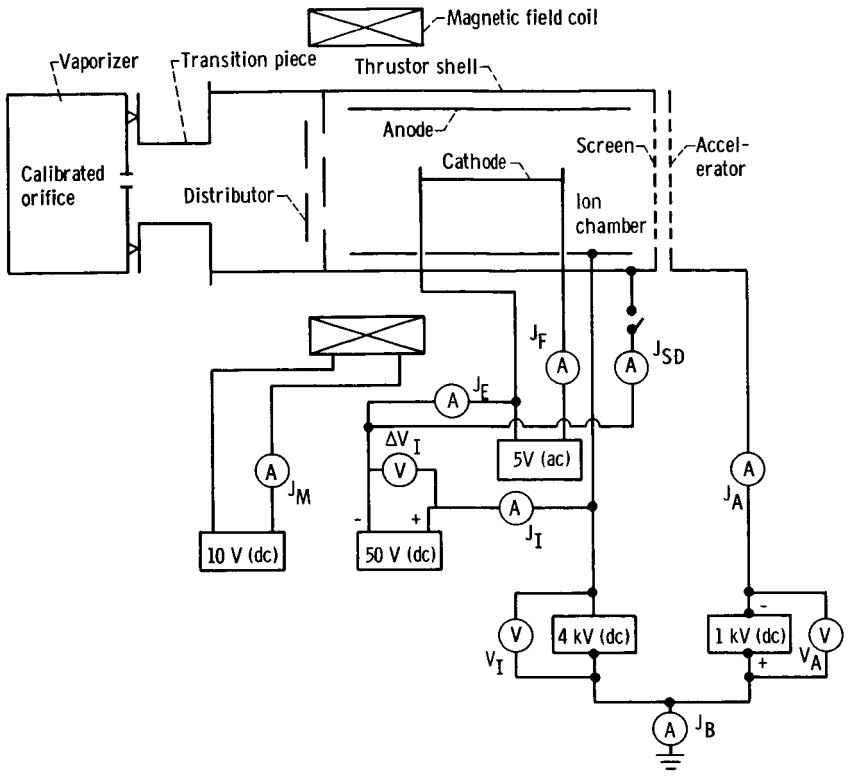

Figure 2. - Wiring diagram of ion thrustor.

sisted of two strands of 0.038-centimeter tantalum wire twisted together. For tests with grid sets 9 and 10, the cathode was a tantalum ribbon. Further construction details are given in tables I and II (pp. 11 and 12).

The electrical circuitry shown in figure 2 has been commonly used in the past to test the thrustor with conventional grids. For operation with the insulated grids, the only circuit change was the electrical isolation of the thrustor shell. This change was accomplished by opening the electrical connection passing through the ammeter (J_{SD} in fig. 2). Primarily, this change was made to minimize electrical breakdowns. Electrical isolation of the thrustor shell had little effect on the thrustor performance for either the conventional or the insulated grids.

Some of the grids that were tested are shown in figure 3. The grid shown in figure 3(a) is a match-drilled set consisting of one ceramic grid and one stainless-steel grid. The ceramic grid was made from a high-temperature, machinable, ceramic mixture of aluminum oxide and a silicon compound. The grids shown in figure 3(b) to (d) consist of various metals onto which 0.02- to 0.05-centimeter thicknesses of aluminum oxide have been vapor deposited by an oxygen-acetylene flame spraying process. Figure 3(e) shows a grid made from a plate of a machinable mica-based ceramic onto which a 0.013-centimeter-thick layer of molybdenum has been vapor deposited. A similar grid was made by using boron nitride coated with electrically conducting paint. The dimen-

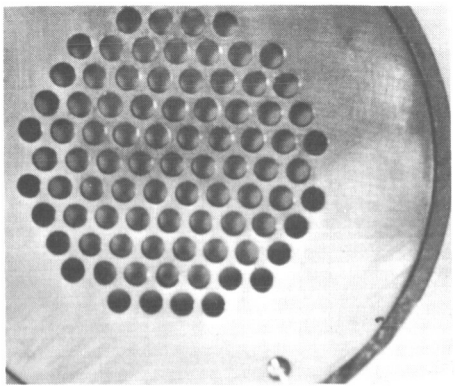

(a) Match-drilled stainless-steel and machinable aluminum oxide (grid set 2, table I).

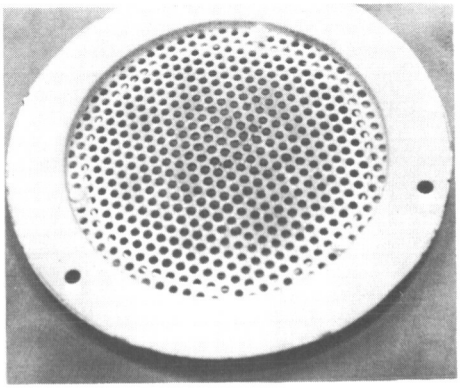

(b) Molybdenum coated with aluminum oxide (grid set 3, table I).

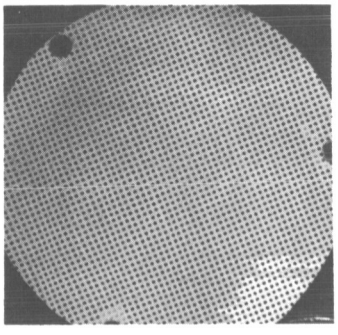

(c) Brass coated with aluminum oxide (grid set 4, table I).

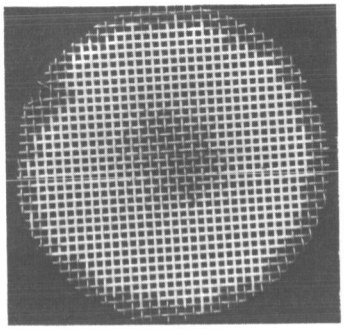

(d) Stainless steel coated with aluminum oxide (grid set 5, table I).

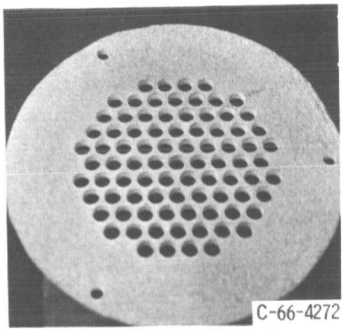

(e) Mica-based ceramic coated with molybdenum (grid set 6, table I).

Figure 3. - Some accelerator grids tested.

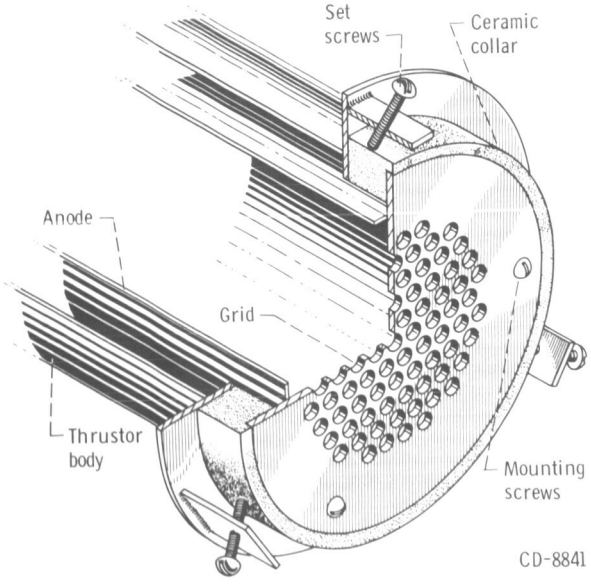

Figure 4. - Method of attachment of insulated grids to thrustor.

sions and compositions of the grids are given in table I (p. 11).

The method by which these insulated grids were attached to the thrustor is shown in figure 4. A ceramic collar was attached to the front of the thrustor and the grids, in turn, were attached to the collar with screws. A photograph of the thrustor with the insulating collar is shown in figure 1. This arrangement was chosen for simplicity of fabrication and ease of grid changing.

RESULTS AND DISCUSSION

Initial tests were conducted with a conventional two-grid system (grid set 1,

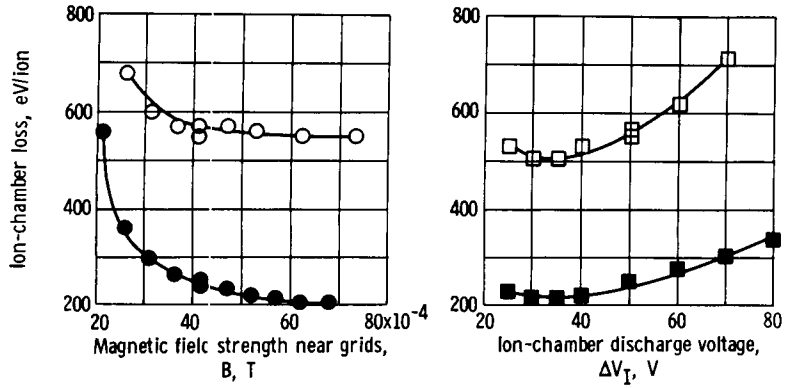

(a) Effect of discharge parameters on ion-chamber loss. Net accelerating voltage, 4000 volts; accelerator voltage, -1000 volts; ion beam current, 0.030 ampere. Unless otherwise noted, discharge voltage, 50 volts; magnetic field strength, 42x10^{-4} tesla.

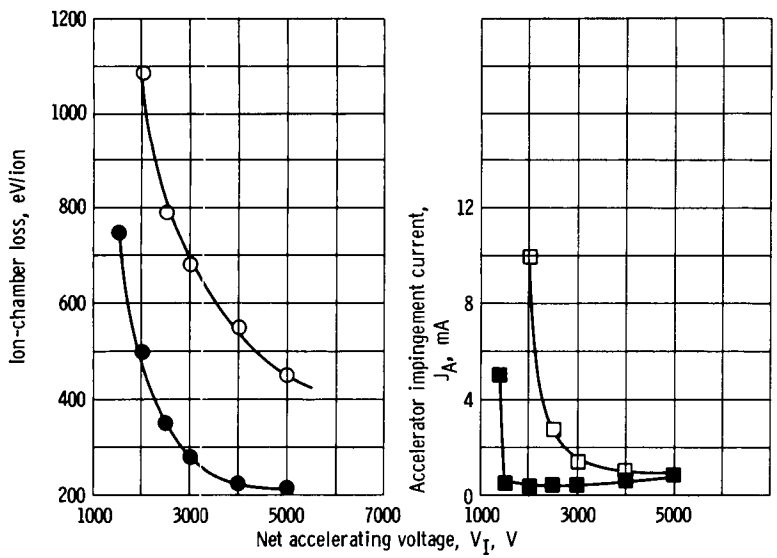

(b) Effect of net accelerating voltage on thrustor performance. Accelerator voltage, -1000 volts; ion beam current, 0.030 ampere; discharge voltage, 50 volts; magnetic field strength, 42x10^{-4} tesla.

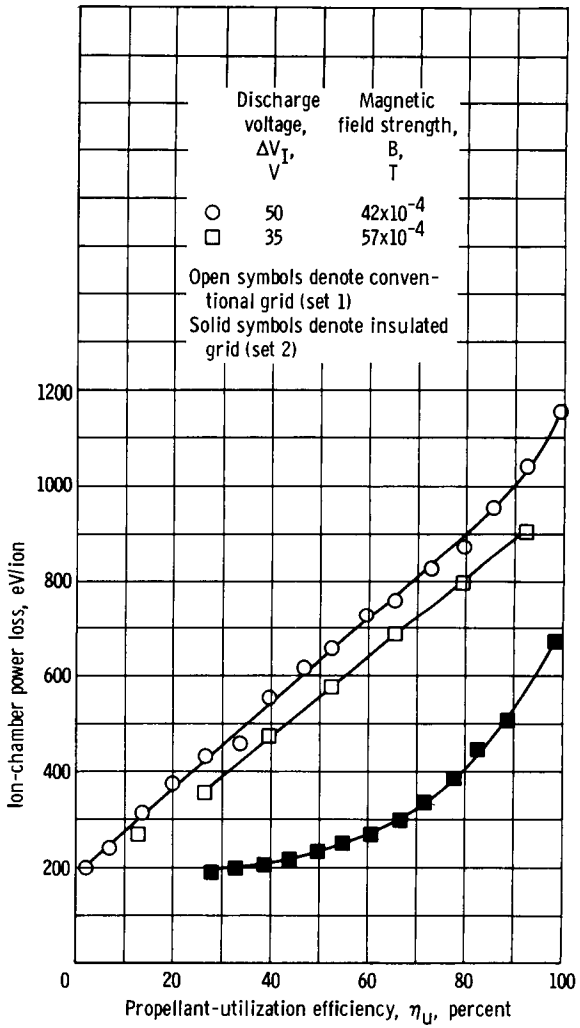

(c) Variation of ion-chamber power loss with propellant-utilization efficiency. Net accelerating voltage, 4000 volts; accelerator voltage, -1000 volts.

Figure 5. - Comparison of ion-chamber performance with conventional grids and with an insulated grid. Neutral propellant flow rates: conventional grids, 0.075 ampere; insulated grid, 0.090 ampere equivalent.

table I, p. 11) to provide a basis for comparison of thrustor performance with the insulated grids. This comparison is shown in figure 5.

Grid set 2 (table I) was designed to provide a comparison with the conventional grids. The ceramic-coated grid matches the conventional screen set in hole diameter (0.476 cm), effective grid spacing (the ceramic thickness, 0.153 cm is comparable to the grid spacing for the original set, 0.134 cm), and thrustor diameter. In figure 5, typical performance data for this ceramic-covered grid are compared with those for the conventional grids. The performance curves show that the insulated grid decreased the ion chamber loss by more than a factor of 2. Otherwise the performance curves of both types of grid exhibit nearly the same trends. In both cases, ion-chamber power loss minimized at a discharge voltage of about 35 volts and at a magnetic field strength (near the grids) of 42×10^{-4} tesla (42 G). The ceramic-coated grid provided low ion-chamber losses and low ion-impingement current over a slightly wider range of net accelerating voltages than did the standard set of grids.

The maximum supportable net accelerating voltage was the same (about 7000 V) for both the conventional and the ceramic-coated sets of grid. In the test of the ceramic-coated grid, an electrical breakdown appeared (from visual observation) to travel from the plasma in the ion chamber through a hole in the ceramic grid to the metal grid.

The maximum supportable electric field strength during thrustor operation was about the same for several grids with varying thicknesses of ceramic insulation. For example, the grid shown in figure 3(b) had a 0.05-centimeter-thick coating of aluminum oxide. The maximum supportable voltage was about 2200 volts. The grid shown in figure 3(a), with a ceramic thickness of about 0.15 centimeter, was able to support a maximum of about 7000 volts. In general, the maximum supportable electric field strength across the ceramic layer was about 3×10^{6} to 6×10^{6} volts per meter, which is approximately the same range as observed previously between conventional grids (refs. 1 and 2).

A summary of the performance of all the grids tested is presented in table II. Grid sets 1 and 2 are compared in figure 5. Grid set 3 had a thin ceramic coating and was designed to study thrustor operation at low net accelerating voltages. Grid set 4 performed only moderately well (350 to 450 eV/ion), which indicated that a grid with a small percentage of open area was not particularly promising. An insulated wire mesh grid, set 5, was tested. It did not provide adequate performance over as wide a range of voltages as did grids with round holes. Grid set 5 failed because the ceramic used was unable to stand the operating temperatures of the ion thrustor (about 350° C). Grid sets 7 and 8, which were similar to grid set 2 but thicker, consisted of a thick ceramic grid backed with metal. These grids were tested to demonstrate operation at the more common values of net accelerating voltage (3000 to 5000 V). Grid sets 9 to 11 are discussed later in this section.

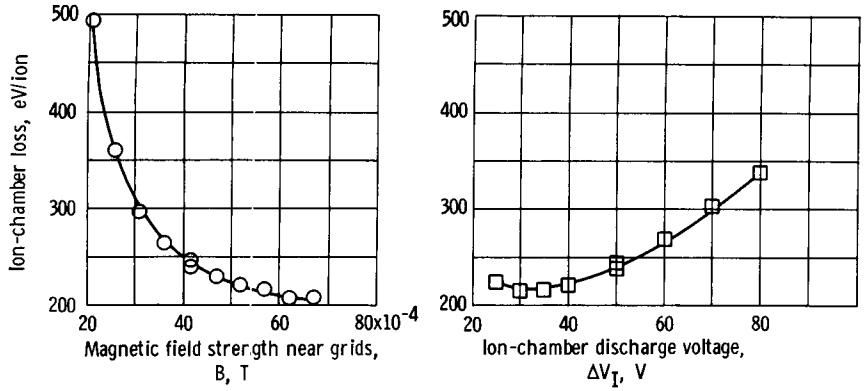

(a) Effect of discharge parameters on ion-chamber loss. Net accelerating voltage, 1500 volts; accelerator voltage, -400 volts; ion beam current, 0.030 ampere. Unless otherwise noted, discharge voltage, 50 volts; magnetic field strength, 42x10^{-4} tesla.

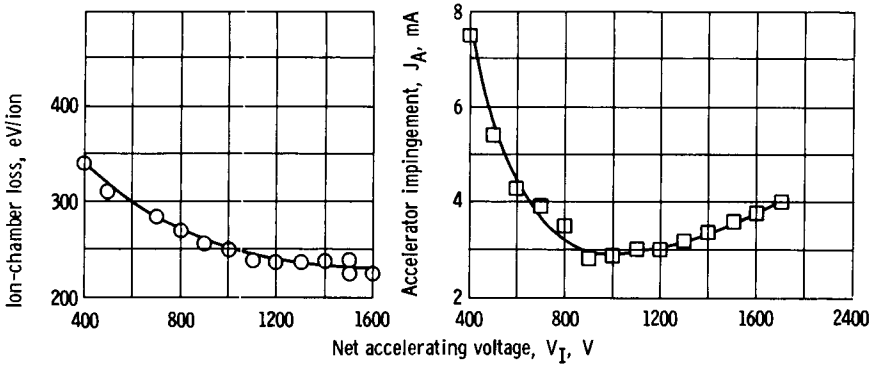

(b) Effect of net accelerating voltage on thrustor performance. Accelerator voltage, -400 volts; ion beam current, 0.030 ampere; discharge voltage, 50 volts; magnetic field strength, 42x10^{-4} tesla.

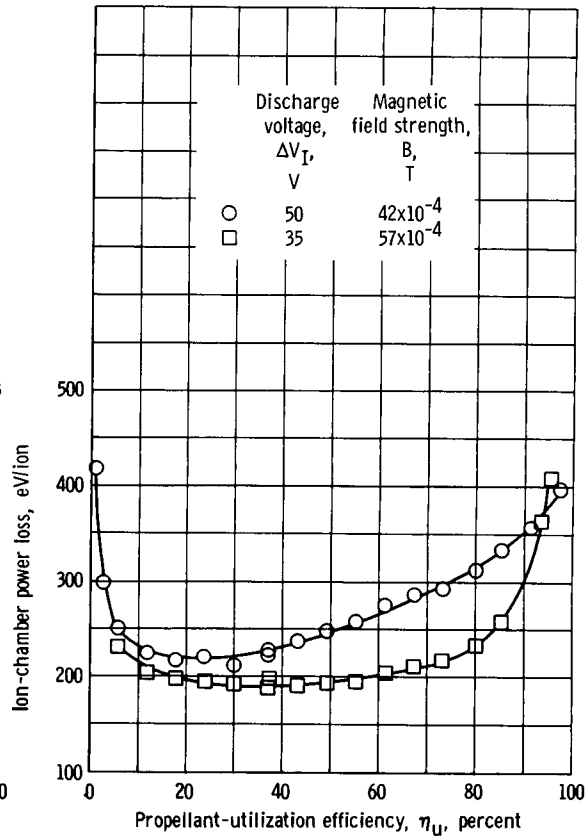

(c) Variation of ion-chamber power loss with propellant-utilization efficiency. Net accelerating voltage, 1500 volts; accelerator voltage, -400 volts.

Figure 6. - Performance of molybdenum grid with aluminum oxide coating. Neutral flow rate, 0.082 ampere equivalent; grid set 3.

The data of figure 6 were obtained with a thinly coated grid (set 3), which might be suitable for use with low-voltage systems. Ion beams were produced at net accelerating voltages as low as 400 volts, with low discharge losses (350 eV/ion), although at a low propellant-utilization efficiency of only 38 percent (ion beam current of 0.030 A). At a net accelerating voltage of 1500 volts, an ion beam with 85-percent-propellant-utilization efficiency was obtained with an ion-chamber loss of only 200 to 250 electron volts per ion. A singly charged mercury ion accelerated through 400 or 1500 volts achieves a velocity corresponding to a specific impulse of 2000 or 3900 seconds, respectively. The thinner coating of insulation that was used for set 3 provided a further decrease in the ion-chamber power loss over grid set 2, which had thicker insulation.

To determine if this accelerator concept was also applicable to larger thrustors, an insulated grid was tested on a 15-centimeter-diameter thrustor. The original two-grid set (grid set 9, tables I and II) allowed operation at an ion beam current of 0.250 ampere, which represents a propellant-utilization efficiency of about 85 percent with an ion-chamber power loss of about 500 electron volts per ion. With an insulated accelerator grid (grid set 10, tables I and II), operation at the same thrustor parameters (i.e., V_I, V_A, ΔV_I, J_B, J_N, J_A, and B) was possible with ion-chamber loss of about 200 electron volts per ion.

In attempting to find an explanation for the improved ion-chamber performance in either size thrustor with the insulated grids, the following possibilities were considered: (1) The layer of insulation on the inner surface of the grid could acquire a surface charge from the ion-chamber plasma that would improve the extraction of ions through the holes in the grids. (2) Extraction of ions might be enhanced because the acceleration distance for each ion is shorter with an insulated grid. In either case, ions that would normally strike the screen grid and be lost might be deflected toward the holes.

If the first explanation (charge distribution on the dielectric) were correct, it should be possible to achieve the same degree of improvement in ion-chamber performance by simply insulating the screen grid of a standard two-grid system. To test this prediction the screen grid of the original set of grids (grid set 1, tables I and II) was coated with aluminum oxide. The resulting grid system (grid set 11, tables I and II) was tested and yielded practically no change in performance from the original configuration. This result rules out significant effects due to the charge distribution on the surface of the dielectric.

If the second explanation (decreased ion acceleration distance) were correct, it would be expected that, for grids comparable in all respects except for the removal of a screen grid, the insulated grid would be capable of accelerating a given beam-current density at a lower voltage. Grid sets 1 and 2 (tables I and II) have the geometric similarities required for a comparison; that is, the metal screen holes are the same diameter as are the accelerator grid holes of the insulated grid, and the space (0.134 cm)

between the metal grids is about the same as the ceramic thickness (0.153 cm) on the insulated grid. From figure 4(b), the minimum operating voltage for the standard grid set (grid set 1) without sharply increased impingement is about 2500 volts (total of 3500 V between the plates). For the comparable insulated grid (grid set 2), the minimum operating voltage is about 1500 volts (total 2500 V between the plasma and the accelerator). The predicted decrease in accelerating voltage for the insulated grid was attained, thus lending some credance to the proposed explanation.

It is an experimental fact (refs. 1 and 2) that, for a standard two-grid set, a thinner screen grid provides a decreased ion-chamber loss. The insulated grids described in this report represent the limiting case of a zero thickness screen grid.

An important question that has not been answered is the durability of the insulated grid compared with a conventional grid pair. During the tests conducted, the grid of figure 3(b) accumulated about 10 hours of operating time with no observable damage. The many thousand hours of durability testing required for a long space mission were considered beyond the scope of this investigation, as was the use of better ceramic-metal bonding techniques in the accelerator grid. The type of construction used was selected for laboratory expendiency.

CONCLUDING REMARKS

Preliminary tests of an electron-bombardment ion thrustor equipped with a single ceramic-protected accelerator indicated that

1. Ion beam extraction of 0.03 ampere in a 5-centimeter-diameter thrustor, was feasible down to a net accelerating voltage of 400 volts with a thinly coated ceramic and small-holed accelerator grid (as might be required in thrustor operation direct from a solar-cell array). This accelerator grid also had the lowest discharge chamber losses (200 to 250 eV/ion) of the entire investigation when operated at net accelerating voltages of 800 to 1500 volts.

2. With the thrustor operating, the maximum supportable field strength across the ceramic layer was approximately constant for the ceramic thicknesses tested (3×10^6 to 6×10^6 V/m), and about equal to that obtainable between two conventional metal grids.

3. General reduction by a factor of 2 occurred in discharge chamber losses when the ceramic-protected grid was compared with a similar, conventional grid system. (Ceramic thickness is equal to the space between the metal grids.) This reduction was realized in both a 5- and a 15-centimeter-diameter thrustor.

4. Other thrustor discharge parameters, that is, optimum magnetic-field strength, optimum chamber discharge voltage, and so forth, were substantially unaffected by use of a single ceramic-protected accelerator grid.

The preliminary investigation of a ceramic-protected accelerator grid indicated that it is a promising approach for the direct-current electron-bombardment thrustor, since it actually resulted in performance increases. Its use in larger diameter thrustors also appeared to be feasible. The ultimate use of this grid in space electric thrustor missions, however, will depend on demonstration of adequate accelerator grid lifetimes.

Lewis Research Center,
National Aeronautics and Space Administration,
Cleveland, Ohio, November 9, 1966,
120-26-02-05-22.

REFERENCES

1. Kerslake, William R.: Accelerator Grid Tests on an Electron-Bombardment Ion Rocket. NASA TN D-1168, 1962.
2. Kerslake, William R.; and Pawlik, Eugene V.: Additional Studies of Screen and Accelerator Grids for Electron-Bombardment Ion Thrustors. NASA TN D-1411, 1963.
3. Sohl, G.; Reid, G. C.; Barcatta, F. A.; Zafran, S.; and Speiser, R. C.: Ion Rocket System Research and Development. Rep. No. EOS-4920-Final (NASA CR-54323), Electro-Optical Systems, Inc., Dec. 1965.
4. Pawlik, Eugene V.; Margosian, Paul M.; and Staggs, John F.: A Technique for Obtaining Plasma-Sheath Configurations and Ion Optics for an Electron-Bombardment Ion Thrustor. NASA TN D-2804, 1965.
5. Freisinger, J.; and Löb, H.: Ein Elektrostatisches Triebwerk Mit Hochfrequenz-Ionenquelle. Paper presented at Wissenschaftliche Gesellschaft für Luft- und Raumfahrt and Deutsche Gesellschaft für Raketentechnik und Raumfahrtforschung, Jahrestagung, Berlin, West Germany, Sept. 14-18, 1964.
6. Keller, Thomas A.: NASA Electric Rocket Test Facilities. Seventh National Symposium on Vacuum Technology Transaction, C. Robert Meissner, ed. Pergamon Press, Inc., 1961, pp. 161-167.
7. Kerslake, William R.; Wasserbauer, Joseph F.; and Margosian, Paul M.: A Mercury Electron-Bombardment Ion Thrustor Suitable for Spacecraft Station Keeping and Attitude Control. Paper No. 66-247, AIAA, Mar. 1966.

TABLE I. - PHYSICAL DESCRIPTION OF GRIDS

Grid set	Screen			Accelerator			Grid separation, cm	Ceramic coating			Grid open area, percent	Thrustor diameter, cm
	Material	Thickness, cm	Hole diameter, cm	Material	Thickness, cm	Hole diameter, cm		Material	Thickness, cm	Hole diameter, cm		
1	Molybdenum	0.170	0.476	Molybdenum	0.175	0.317	0.134	----------	-----	-----	~46	5
[a]2	----------	-----	-----	Stainless steel	.075	.476	-----	Machinable aluminum oxide	0.153	0.476	~46	5
[b]3	----------	-----	-----	Molybdenum	.090	.218	-----	Aluminum oxide	~.05	.218	37	5
[c]4	----------	-----	-----	Brass	.053	.078	-----	Aluminum oxide	~.02	.078	17	5
[d]5	----------	-----	-----	Stainless-steel mesh	.191	.208	-----	Aluminum oxide	~.025	.208	54	5
[e]6	----------	-----	-----	Ceramic coated with molybdenum	.013	.476	-----	Mica-based ceramic	.318	.476	~46	5
[f]7	----------	-----	-----	Stainless steel	.075	.476	-----	Boron nitride	.320	.476	~46	5
8	----------	-----	-----	Silver paint	~.013	.476	-----	Boron nitride	.213	.476	~46	5
9	Molybdenum	.210	.476	Molybdenum	.25	.317	.302	----------	-----	-----	~50	15
10	----------	-----	-----	Molybdenum	.25	.317	-----	Boron nitride	.153	.317	~50	15
[g]11	Molybdenum	.170	.476	Molybdenum	.175	.317	.134	Aluminum oxide	~.025	.476	~46	5

[a]See fig. 3(a).
[b]See fig. 3(b).
[c]See fig. 3(c).
[d]See fig. 3(d).
[e]See fig. 3(e).
[f]Similar to grid set 2 with thicker ceramic plate.
[g]Screen grid coated with ceramic; accelerator grid, bare metal.

TABLE II. - SUMMARY OF PERFORMANCE

Grid set	Thrustor conditions						Propellant-utilization efficiency, η_u, percent			Average fraction of impingement, J_A/J_B at η_u = 60 percent	Maximum supportable V_I at indicated V_A, V
	Magnetic field strength, B, T		Net accelerating voltage, V_I, V	Accelerator voltage, V_A, V	Discharge voltage, V_I, V	Neutral propellant flow rate, J_N, A	30	60	85		
	Distributor	Grid					Ion-chamber power loss, eV/ion				
1	63×10^{-4}	42×10^{-4}	4000	-1000	50	0.075	475	710	930	0.04	6000
	86	57	4000	-1000	35	.075	415	625	850	.04	----
[a]2	63×10^{-4}	42×10^{-4}	4000	-1000	50	0.090	215	305	430	0.012	6000
	86	57	4000	-1000	35	.090	190	270	460	.012	----
[b]3	63×10^{-4}	42×10^{-4}	1800	-400	50	0.180	290	500	---	0.08	2000
	63	42	1500	-400	50	.082	225	270	330	.055	----
	86	57	1500	-400	35	.082	190	205	250	.055	----
[c]4	63×10^{-4}	42×10^{-4}	1500	-400	50	0.075	305	440	550	0.30	1600
	86	57	1500	-400	35	.075	245	325	450	.30	----
[d]5	63×10^{-4}	42×10^{-4}	1500	-400	50	0.075	275	375	480	0.13	1800
	86	57	1500	-400	50	.075	250	307	400	.13	----
7	63×10^{-4}	42×10^{-4}	4000	-1000	50	0.075	300	390	720	0.008	7000
	86	57	4000	-1000	35	.075	200	265	---	.007	----
8	63×10^{-4}	42×10^{-4}	4000	-1000	50	0.087	235	255	320	0.072	7000
	86	57	4000	-1000	40	.087	190	210	300	.044	----
	63	42	1800	-1000	50	.087	270	450	---	.034	----
[e]9	36×10^{-4}	16×10^{-4}	3000	-2000	50	0.305	285	390	500	0.013	5000
[e]10	36×10^{-4}	16×10^{-4}	3000	-2000	50	0.300	130	142	190	0.012	----
[f]11	63×10^{-4}	42×10^{-4}	4000	-1000	50	0.075	600	750	960	0.04	6000

[a]See fig. 3(a).
[b]See fig. 3(b).
[c]See fig. 3(c).
[d]See fig. 3(e).
[e]Permanent magnet; 15-cm-diam thrustor, tantalum ribbon cathode as in ref. 2.
[f]Same as grid set 1 with screen grid coated with ceramic.

"The aeronautical and space activities of the United States shall be conducted so as to contribute . . . to the expansion of human knowledge of phenomena in the atmosphere and space. The Administration shall provide for the widest practicable and appropriate dissemination of information concerning its activities and the results thereof."

—NATIONAL AERONAUTICS AND SPACE ACT OF 1958

NASA SCIENTIFIC AND TECHNICAL PUBLICATIONS

TECHNICAL REPORTS: Scientific and technical information considered important, complete, and a lasting contribution to existing knowledge.

TECHNICAL NOTES: Information less broad in scope but nevertheless of importance as a contribution to existing knowledge.

TECHNICAL MEMORANDUMS: Information receiving limited distribution because of preliminary data, security classification, or other reasons.

CONTRACTOR REPORTS: Technical information generated in connection with a NASA contract or grant and released under NASA auspices.

TECHNICAL TRANSLATIONS: Information published in a foreign language considered to merit NASA distribution in English.

TECHNICAL REPRINTS: Information derived from NASA activities and initially published in the form of journal articles.

SPECIAL PUBLICATIONS: Information derived from or of value to NASA activities but not necessarily reporting the results of individual NASA-programmed scientific efforts. Publications include conference proceedings, monographs, data compilations, handbooks, sourcebooks, and special bibliographies.

Details on the availability of these publications may be obtained from:

SCIENTIFIC AND TECHNICAL INFORMATION DIVISION

NATIONAL AERONAUTICS AND SPACE ADMINISTRATION

Washington, D.C. 20546